Taurine treatment of retinal degeneration and cardiomyopathy in a consanguineous family with SLC6A6 taurine transporter deficiency

Muhammad Ansar[1,2,§,*], Emmanuelle Ranza[1,3,4,§], Madhur Shetty[5], Sohail A. Paracha[6], Maleeha Azam[7], Ilse Kern[8], Justyna Iwaszkiewicz[9], Omer Farooq[10], Constantin J. Pournaras[11], Ariane Malcles[12], Mateusz Kecik[12], Carlo Rivolta[13,14,15], Waqar Muzaffar[16], Aziz Qurban[16], Liaqat Ali[7], Yacine Aggoun[17], Federico A. Santoni[1,18], Periklis Makrythanasis[1,19], Jawad Ahmed[6], Raheel Qamar[7], Muhammad T. Sarwar[6], L. Keith Henry[5], Stylianos E. Antonarakis[1,3,20,*]

[1]Department of Genetic Medicine and Development, University of Geneva, Geneva, Switzerland;

[2]Current address, Clinical Research Center, Institute of Molecular and Clinical Ophthalmology Basel (IOB), Basel, Switzerland;

[3]Service of Genetic Medicine, University Hospitals of Geneva, Geneva, Switzerland;

[4]Current address, Medigenome, Swiss Institute of Genomic Medicine, Geneva, Switzerland;

[5]Dept. of Biomedical Sciences, School of Medicine and Health Sciences, University of North Dakota, Grand Forks, ND, United States;

[6]Institute of Basic Medical Sciences, Khyber Medical University, Peshawar, Pakistan;

[7]Department of Biosciences, Faculty of Science, COMSATS University Islamabad, Pakistan;

[8]Pediatric Nephrology and Metabolism Unit, Pediatric Subspecialties Service, Children's Hospital, Geneva University Hospitals, Geneva, Switzerland;

[9]Swiss Institute of Bioinformatics, Molecular Modeling Group, University of Lausanne, Lausanne, Switzerland;

[10]Bahria University Medical and Dental College, Karachi, Pakistan;

[11]Hirslanden Clinique La Colline, Geneva, Switzerland ;

[12]Department of Ophthalmology, University Hospitals of Geneva, Geneva, Switzerland;

[13]Clinical Research Center, Institute of Molecular and Clinical Ophthalmology Basel (IOB), Basel, Switzerland;

[14]Department of Ophthalmology, University Hospital Basel, Switzerland;

[15]Department of Genetics and Genome Biology, University of Leicester, Leicester, United

[16]Armed Forces Institute of Ophthalmology, Rawalpindi, Pakistan;

[17]Pediatric Cardiology, Geneva University Hospitals, Geneva, Switzerland;

[18]Current address, Department of Endocrinology Diabetes and Metabolism, University Hospital of Lausanne, Lausanne, Switzerland;

[19]Current address, Biomedical Research Foundation of the Academy of Athens, Athens, Greece;

Kingdom;

[20]iGE3 Institute of Genetics and Genomics of Geneva, Geneva, Switzerland;

[§]These authors contributed equally

[*]Corresponding authors;

Muhammad Ansar

University of Geneva Medical School, 1 Rue Michel Servet, 1211 Geneva, Switzerland

Phone: +41 78 805 5480

Fax: +41-22-379-5706

muhammad.ansar@unige.ch

Current address, Clinical Research Center, Institute of Molecular and Clinical Ophthalmology Basel (IOB), Basel, Switzerland.

muhammad.ansar@iob.ch

Stylianos Antonarakis

University of Geneva Medical Faculty, 1 Rue Michel Servet, 1211 Geneva, Switzerland

Phone: +41 22 37 95708

Fax: +41-22-379-5706

stylianos.antonarakis@unige.ch

Abstract

In a consanguineous Pakistani family with 2 affected individuals, a homozygous variant Gly399Val in the 8th transmembrane domain of the taurine transporter SLC6A6 was identified resulting in a hypomorph transporting capacity of ~15% compared to normal. 3D modeling of this variant has indicated that it likely causes displacement of the Tyr138 (TM3) side chain, important for transport of taurine. The affected individuals presented with rapidly progressive childhood retinal degeneration, cardiomyopathy, and almost undetectable plasma taurine levels. Oral taurine supplementation of 100mg/kg/day resulted in maintenance of normal blood taurine levels. Following approval by the ethics committee, a long-term supplementation treatment was introduced. Remarkably, after 24-months, the cardiomyopathy was corrected in both affected siblings, and in the 6 y.o. the retinal degeneration was arrested, and the vision was clinically improved. Similar therapeutic approaches could be employed in mendelian phenotypes caused by the dysfunction of the hundreds of other molecular transporters.

Introduction

Transporters constitute a large number of cell membrane proteins involved in the uptake of small molecules into cells(1). The current human gene catalogue contains 423 protein-coding genes classified as solute carrier (SLC)(1) (https://www.genenames.org/data/genegroup/#!/group/752). Members of this large gene family are involved in a number of human disorders; OMIM contains 268 entries with dominant, recessive, and X-linked mendelian phenotypes caused by pathogenic variants in these genes (24sep19 search https://www.omim.org/).

Genome or exome sequencing provided the opportunity to identify novel causative links between pathogenic variants of genes and mendelian phenotypes. This is particularly important for the discovery of novel autosomal recessive genes since the majority of those are still unknown. Consanguinity, which is practiced in a considerable fraction of world's populations, provides a means to identify novel recessive genes because of the large genomic regions of homozygosity in the offspring of closely related parents(2). The identification of pathogenic variants in novel genes causing recessive disorders provide a better understanding of the molecular pathophysiology of the resulting phenotype, and the opportunity for improved diagnostic services to the affected families and populations; occasionally, new therapeutic options could be offered based on the underlying molecular mechanism.

As part of the Swiss-Pakistani consanguinity project, to identify novel genes for visual impairment or intellectual disability(3, 4), we present a novel gene for childhood progressive retinal degeneration and cardiomyopathy in one family. The taurine transport defect identified due to a hypomorph homozygous pathogenic variant in the SLC6A6 gene, has provided the opportunity for treatment with long-term taurine supplementation. After 24 months of treatment the

cardiomyopathy was corrected in both affected siblings, and in the 6 y.o. the retinal degeneration was arrested and the vision was clinically improved.

Results

Genetic analysis

We used exome sequencing and genotyping of more than 200 Pakistani consanguineous families with multiple affected individuals to identify candidate genes and high impact variants responsible for recessive visual impairment. In one of these consanguineous families, F315, from the Kohat region of Pakistan with 2 affected individuals, we have identified a homozygous deleterious variant Gly399Val (NM_003043.5:c.1196G>T) in the taurine transporter SLC6A6 (MIM:186854) that segregated with the phenotype of progressive retinal degeneration (Figure 1A, 1B). Gly399 of SLC6A6 is well-conserved in all vertebrates (Figure 1C), and 3D molecular modeling (Figure 1D) predicted that the Val399 substitution causes a displacement of Tyr138 side chain, important for the recognition and transport of the ligand. Blood taurine levels in the two affected individuals IV:1 and IV:3 were almost undetected (6-7 μmol/l).

Functional analysis

Transient and stable transfection of the Gly399Val variant in HEK-293 cells resulted in a hypomorph with transport capacity of ~15% compared to normal as determined by single point (Figure S2) and saturation (Figure S3 and Table S6) radioactive taurine uptake analyses. Fibroblasts from affected and carrier individuals of the family showed similar results where single point uptake revealed significant taurine uptake deficits in the affected individuals compared to carriers (Figure S4) consistent with kinetic data showing a significant reduction in V_{MAX} (Figure 2A and Table S7). Plasma membrane expression analysis in HEK-293 cells and fibroblasts strongly support that the transport deficit is functional rather than a result of decreased surface protein (Figure S5 and Figure 2 panels B and C). In HEK-293 cells, taurine transport K_M values

were 3.4-fold lower in SLC6A6 Gly399Val compared to the normal transporter (Table S5) and whereas this could contribute to decreased transport capacity in HEK cells, K_M values were unchanged between affected and carrier fibroblasts (Table S7) indicating the reduced taurine uptake in the affected patients originates from reduced transporter cycling and not substrate recognition.

Clinical evaluation

Clinical examinations in the University Hospitals of Geneva revealed a cone-rod retinopathy and cardiomyopathy. The older 15 y.o. male IV:1 had light perception vision due to advanced macular atrophy with severe peripheral alterations including pseudoosteoblast formation and peripheral atrophy. There was no retinal response in the electroretinogram (ERG) and extensive loss of photoreceptors was noted in the optical coherence tomography (OCT). The younger 6 y.o. female IV:3 had vision of counting fingers due to foveal-spearing macular atrophy. There were less marked peripheral retinal changes (salt-and-pepper fundus pigmentation), no response in global ERG, and minimal electrical focal macular response in the multifocal ERG. The OCT showed atrophy of the photoreceptors with persistence of residual photoreceptors in the central area (Figure S1). Echocardiography showed mild hypokinetic cardiomyopathy in both affected individuals with systolic dysfunction (shortening fraction 24-27%) and systolic dilatation of the left ventricle (Figure 3B); the effort test was however within normal limits. In both patients, brain MRI and hepatic ultrasound was normal (Table S1). Plasma amino acids showed very low levels of taurine in the affecteds and intermediate levels in the carrier parents (Figure 3A).

Taurine supplementation treatment

The oral taurine loading test and subsequent supplementation at 100mg/kg/day resulted in maintenance of normal blood taurine levels in both affected individuals (more than 40 µmol/l in each patient) (Figure S6, Figure 3A). We hypothesized that taurine administration may be beneficial in this family. Following approval by the ethics committee of the University Hospitals of Geneva (protocol #CER 11-036), a long-term oral supplementation treatment of 100mg/kg/day taurine divided in 3 doses was introduced upon return of the family to Pakistan. Remarkably, after 24 months of treatment, the cardiomyopathy was corrected in both affected siblings. The heart function objectified by echocardiography measurements were within normal limits; indicatively, the fractional shortening of the left ventricle in both affected children was 32% (normal range of 30-40%) (Figure 3B). In the female IV:3 (now 8 y.o.) we have noted an improved visual performance with the visual acuity of 20/100 in the right eye and 20/160 in the left eye, while the ophthalmological exams showed stability of the anatomy of the central retina, suggesting an arrest in the further degeneration of the retina (Figure 1C, 1D). Note that the elder brother (IV:1) had a complete visual loss at the age of 8-years. No side effects from the taurine supplementation were noted, as previously reported(5).

Discussion

Taurine is the most abundant amino acid in the retina, important in photoreceptor survival and protection from oxidative stress and light damage(6, 7). Mice with targeted disruption of the Taut/Slc6a6 gene develop degenerative retinal disease(8) similar to that observed in the family F315. Furthermore, chemically-induced taurine deficiency in mice following a treatment with a taurine transporter inhibitor guanidoethane sulfonate, resulted in photoreceptor degeneration and retinal ganglion cell loss(7, 9, 10). In addition, taurine deficiency in cats and dogs(11) causes cardiomyopathy(12). Dogs diagnosed with taurine deficiency and dilated cardiomyopathy had significant improvement in their echocardiographic parameters and normalization of taurine concentrations following diet change and taurine supplementation(11).

In this study we present a family with taurine deficiency due to a homozygous amino acid substitution in third transmembrane domain (TM3) of the taurine transporter SLC6A6. The identification of the functional defect of the taurine transporter SLC6A6 in this consanguineous family which altered taurine homeostasis provided an opportunity for treatment. Two years of oral taurine supplementation resulted in complete reversal of the systolic cardiomyopathy in both affected children, and non-progression of the retinopathy in the younger sibling. We propose the continuation of the taurine supplementation with the objective to stabilize the retinal damage. Additional families with this novel SLC6A6 retinopathy and cardiomyopathy are necessary to establish the therapeutic value of oral taurine supplementation. This study emphasizes the contribution of each novel mendelian gene in the understanding of disease etiology, and provides the opportunity to investigate nutritional or pharmaceutical therapy for severe mendelian disorders due to the large family of 423 transporter-encoding genes(1). In addition, the identification of

novel genes for autosomal recessive disorders provides the opportunity for carrier detection in the extended pedigree and family planning.

Materials and Methods

Family ascertainment

Family (F315) was ascertained and sampled by the Institute of Basic Medical Sciences (IBMS), Khyber Medical University, Peshawar, Pakistan and was studied at the Department of Genetic Medicine and Development, University of Geneva, Switzerland. The study was approved by the ethical committee of the Khyber Medical University, Peshawar, Pakistan and by the Bioethics Committee of the University Hospitals of Geneva (Protocol number: CER 11-036). Informed consent was signed by the guardians of this family. Blood samples were obtained from all individuals of the family including affecteds, unaffected siblings and both parents. Genomic DNA was extracted from blood samples.

Genetic analysis

Exome sequencing of the proband (IV:3) was performed as described previously(13). All the family members including affecteds (IV:1 and IV:3), unaffected siblings (IV:4 and IV:5) and both parents (III:3 and III:4) were genotyped to identify the runs of homozygosity (ROH). Screening of all the ROHs segregating with the disease phenotype, identifying variants from the exome sequencing present in the segregating ROHs, and filtering of the selected variants were performed by using CATCH(14). Filtering and prioritization of likely pathogenic variants was performed as described previously(4, 13). All candidate variants were validated by Sanger sequencing (Figure 1B).

[^{3}H Taurine] Uptake Assay and Surface Biotinylation

Human embryonic kidney (HEK-293) cell lines were transfected with standard TransIT-LT1 protocol to stably express either wildtype taurine transporter SLC6A6 (formerly called TauT) or a SLC6A6 containing the SNP Glu399Val. HEK-293 cells transiently transfected or stably expressing SLC6A6 or the Glu399Val mutation (100,000 cells/well) or primary fibroblasts (50,000 cells/well) were plated in a 24 well culture plate (culturplate-24, Perkin-Elmer, Inc) and grown for 24 h. Single point uptake of 30 nM or 5 μM [3H] taurine (Perkin Elmer) with vehicle or indicated concentrations of cold taurine was carried out for 10 minutes at 37˚C. 5 μM was obtained by mixing [^{3}H] taurine with non-labeled taurine. Uptake was terminated with three washes of ice-cold KR buffer of pH 7.4. Radioactivity remaining in cells was measured by liquid scintillation. Non-specific uptake was determined for HEK-293 cells by subtracting radioactivity obtained with parental, non-transfected cells. Non-specific uptake for primary fibroblasts was determined by uptake in the presence of 25 mM non-labeled β-alanine. For saturation analysis, [^{3}H] taurine was diluted into non-labeled taurine to obtain the necessary concentrations. Statistical significance was determined using unpaired T-Test and one-way ANOVA (post-Tukey Test) with significance set at $p < 0.05$.

The protocol for surface biotinylation is described in the supplementary data. SLC6A6 expression was normalized to TFRC for each sample.

Taurine loading test and supplementation

A taurine loading test was performed in the Pediatrics clinical research unit of the University hospitals of Geneva after approval by the ethics committee. We have administered an oral bolus dose of 100mg/kg of Taurine to the two affected individuals and their heterozygous parents on day 2, as this dose was recommended by the literature as non-toxic(5). Taurine was provided in tablets,

commercialized by Burgerstein Pharmaceuticals. Repeated measurements of taurine in blood and urine were subsequently performed. On days 3 and 4, the patients received a 100mg/kg/day, administered in 3 doses (33mg/kg/q8hours).

Acknowledgements

We thank the grants from the ProVisu foundation and ERC 219968 to S.E.A., and NIH DA027845 to L.K.H. We thank the family members for their contribution and Mr. M. Akbar for assistance. We thank F. Sloan Bena, J. Fluss, H. Cao Van, S. Hanquinet, F. Marechal and M. Rodriguez, for clinical care and laboratory assistance.

Competing interests

The authors declare no competing interests.

References

1 Hediger, M.A., Clemencon, B., Burrier, R.E. and Bruford, E.A. (2013) The ABCs of membrane transporters in health and disease (SLC series): introduction. *Mol Aspects Med*, **34**, 95-107.

2 Hamamy, H., Antonarakis, S.E., Cavalli-Sforza, L.L., Temtamy, S., Romeo, G., Kate, L.P., Bennett, R.L., Shaw, A., Megarbane, A., van Duijn, C. *et al.* (2011) Consanguineous marriages, pearls and perils: Geneva International Consanguinity Workshop Report. *Genet Med*, **13**, 841-847.

3 Ansar, M., Chung, H.L., Taylor, R.L., Nazir, A., Imtiaz, S., Sarwar, M.T., Manousopoulou, A., Makrythanasis, P., Saeed, S., Falconnet, E. *et al.* (2018) Bi-allelic Loss-of-Function Variants in DNMBP Cause Infantile Cataracts. *Am J Hum Genet*, **103**, 568-578.

4 Ansar, M., Ullah, F., Paracha, S.A., Adams, D.J., Lai, A., Pais, L., Iwaszkiewicz, J., Millan, F., Sarwar, M.T., Agha, Z. *et al.* (2019) Bi-allelic Variants in DYNC1I2 Cause Syndromic Microcephaly with Intellectual Disability, Cerebral Malformations, and Dysmorphic Facial Features. *Am J Hum Genet*, **104**, 1073-1087.

5 Ghandforoush-Sattari, M., Mashayekhi, S., Krishna, C.V., Thompson, J.P. and Routledge, P.A. (2010) Pharmacokinetics of oral taurine in healthy volunteers. *J Amino Acids*, **2010**, 346237.

6 Froger, N., Moutsimilli, L., Cadetti, L., Jammoul, F., Wang, Q.P., Fan, Y., Gaucher, D., Rosolen, S.G., Neveux, N., Cynober, L. *et al.* (2014) Taurine: the comeback of a neutraceutical in the prevention of retinal degenerations. *Prog Retin Eye Res*, **41**, 44-63.

7 Froger, N., Jammoul, F., Gaucher, D., Cadetti, L., Lorach, H., Degardin, J., Pain, D., Dubus, E., Forster, V., Ivkovic, I. *et al.* (2013) Taurine is a crucial factor to preserve retinal ganglion cell survival. *Adv Exp Med Biol*, **775**, 69-83.

8 Warskulat, U., Heller-Stilb, B., Oermann, E., Zilles, K., Haas, H., Lang, F. and Haussinger, D. (2007) Phenotype of the taurine transporter knockout mouse. *Methods Enzymol*, **428**, 439-458.

9 Gaucher, D., Arnault, E., Husson, Z., Froger, N., Dubus, E., Gondouin, P., Dherbecourt, D., Degardin, J., Simonutti, M., Fouquet, S. *et al.* (2012) Taurine deficiency damages retinal neurones: cone photoreceptors and retinal ganglion cells. *Amino Acids*, **43**, 1979-1993.

10 Hadj-Said, W., Froger, N., Ivkovic, I., Jimenez-Lopez, M., Dubus, E., Degardin-Chicaud, J., Simonutti, M., Quenol, C., Neveux, N., Villegas-Perez, M.P. *et al.* (2016) Quantitative and Topographical Analysis of the Losses of Cone Photoreceptors and Retinal Ganglion Cells Under Taurine Depletion. *Invest Ophthalmol Vis Sci*, **57**, 4692-4703.

11 Kaplan, J.L., Stern, J.A., Fascetti, A.J., Larsen, J.A., Skolnik, H., Peddle, G.D., Kienle, R.D., Waxman, A., Cocchiaro, M., Gunther-Harrington, C.T. *et al.* (2018) Taurine deficiency and dilated cardiomyopathy in golden retrievers fed commercial diets. *PLoS One*, **13**, e0209112.

12 Pion, P.D., Kittleson, M.D., Rogers, Q.R. and Morris, J.G. (1987) Myocardial failure in cats associated with low plasma taurine: a reversible cardiomyopathy. *Science*, **237**, 764-768.

13 Makrythanasis, P., Nelis, M., Santoni, F.A., Guipponi, M., Vannier, A., Bena, F., Gimelli, S., Stathaki, E., Temtamy, S., Megarbane, A. *et al.* (2014) Diagnostic exome sequencing to elucidate the genetic basis of likely recessive disorders in consanguineous families. *Hum Mutat*, **35**, 1203-1210.

14 Santoni, F.A., Makrythanasis, P. and Antonarakis, S.E. (2015) CATCHing putative causative variants in consanguineous families. *BMC Bioinformatics*, **16**, 310.

Figure Legends

Figure1. The segregation, conservation and 3D modeling of the SLC6A6 pathogenic variant Gly399Val in family F315 (A) Pedigree of consanguineous family F315 showing the segregation of the homozygous pathogenic variant NM_003043.5:c.1196G>T:p.(Gly399Val) in the SLC6A6 gene. **(B)** Chromatograms of Sanger sequencing showing the segregation of the *SLC6A6* variant c.1196G>T:p.(Gly399Val) in all family members tested. **(C)** Amino acid alignment in various species showing that Gly399 is well conserved. **(D)** Molecular modeling of the SLC6A6 variant Gly399Val indicating that Val399 is predicted to cause the displacement of the Tyr138 (TM3) side chain, which is important for recognition and transport of the ligand.

Figure2. Functional characterization of SLC6A6 activity from patient-derived fibroblasts. (A) Specific Taurine Saturation Uptake Analysis in Patient-derived Fibroblasts. Fibroblasts of affected individuals IV:1 (filled circle), IV:3(open circle), and parents III:3 (closed square) and III:4 (open square) were incubated with [^{3}H] taurine concentrations from 0.05 to 250 μM for 10 min. Non-specific counts were determined by inhibition of SLC6A6 with β-alanine (25 mM) and subtracted from total counts. **(B)** Western Blot detection of SLC6A6 in the plasma membrane from patient-derived fibroblasts. Surface protein was purified through biotinylation with a cell impermeant crosslinker and detected using anti-SLC6A6 antibody. **(C)** Percent surface expression was calculated from band densitometry for each sample and normalized to TFRC and plotted. * $P<0.05$

Figure3. Results of taurine supplementation therapy for 24-months (A) Taurine levels in the blood of both affected individuals (IV:1 and IV:3) before and after 6-months, 1-year and 2-years of taurine supplementation. **(B)** Results of the echocardiography show that the cardiomyopathy of

both affected individuals (IV:1 and IV:3) has been corrected after 2-years of taurine supplementation. LVESD: left ventricular end-systolic diameter, LVEDD: left ventricular end diastolic diameter, EF: ejection fraction, FS: fractional shortening. Green and red numbers represent normal and abnormal values respectively. **(C, D)** Fundus photographs and macular OCT of the right eye (C) and left eye (D) of the patient IV:3 at baseline and after 24 months of taurine supplementation; anatomical stability with preservation of foveal photoreceptors can be noted.

Figure 1

A

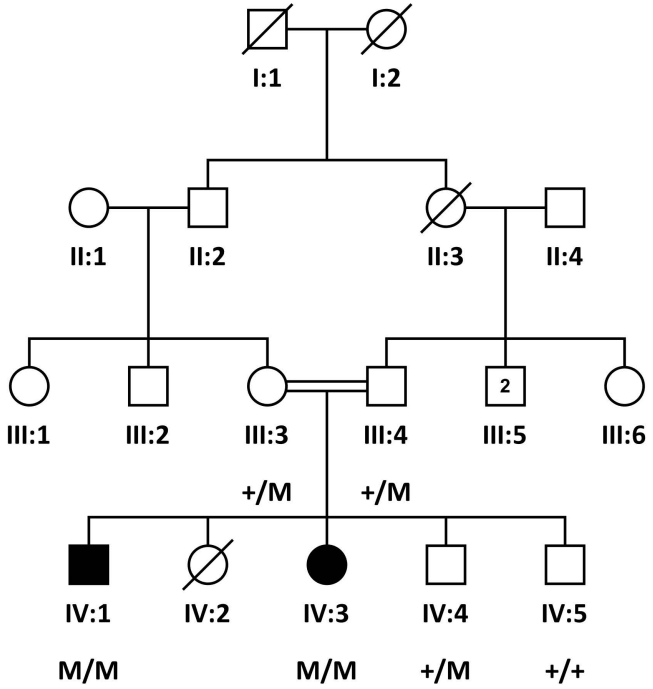

B

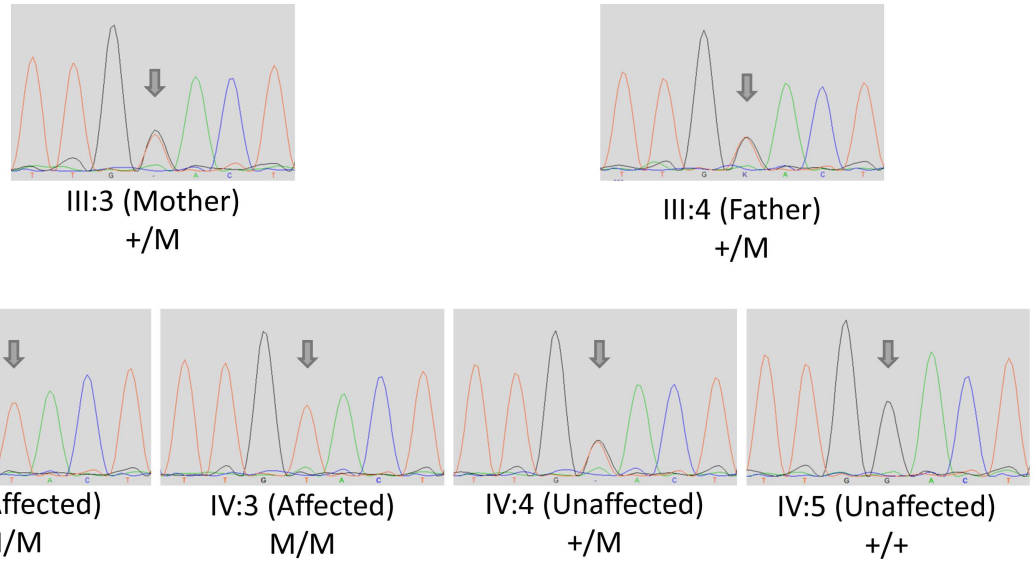

C

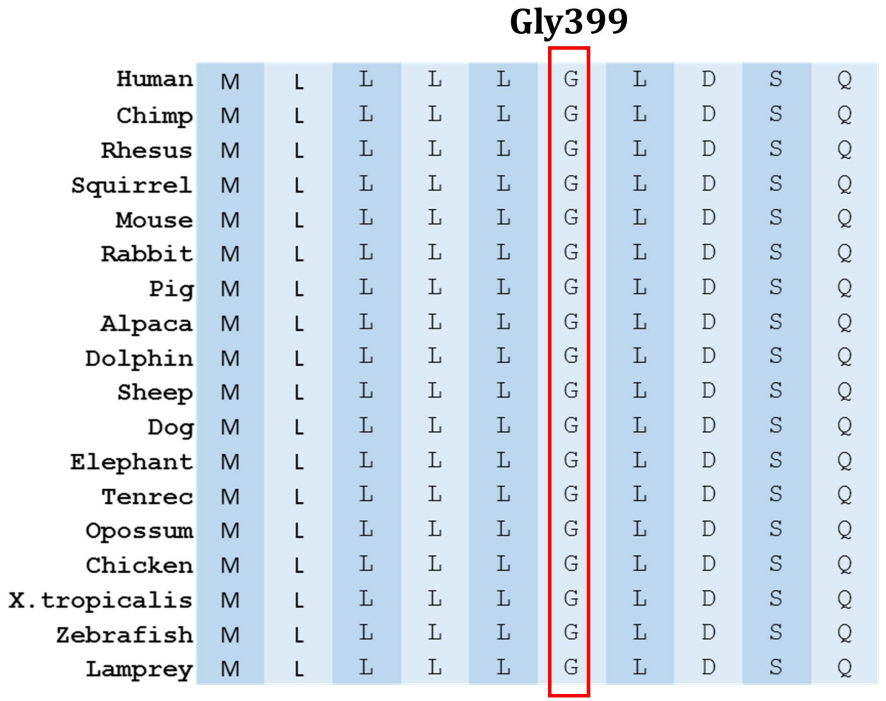

D

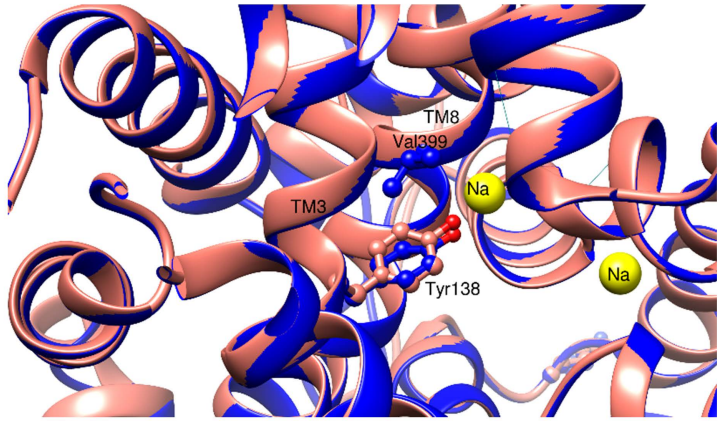

M: SLC6A6:NM_003043.5:c.1196G>T:p.(Gly399Val)

Figure 2

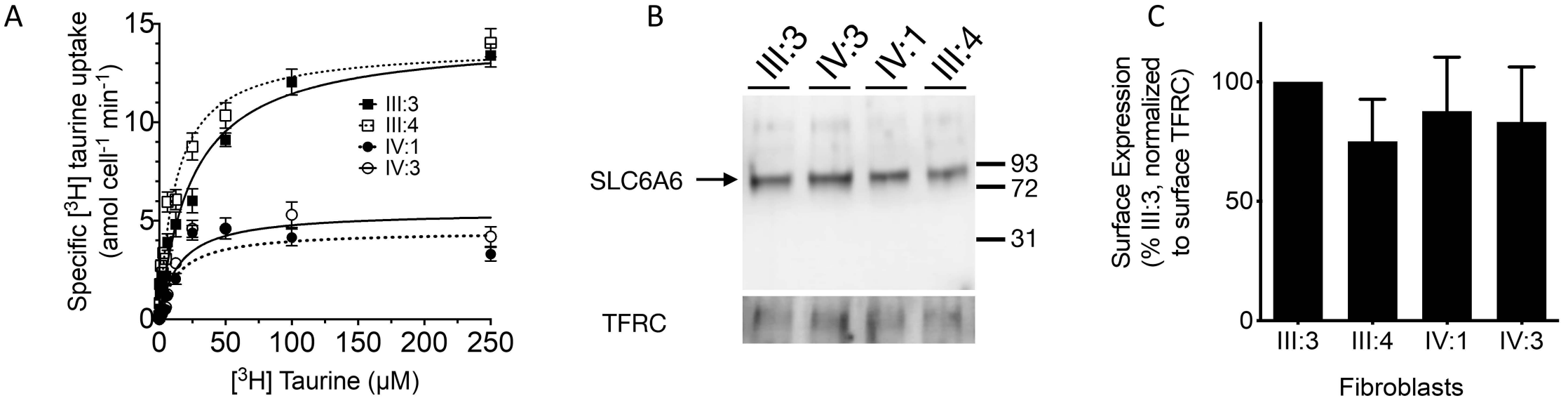
A
Specific [3H] taurine uptake (amol cell-1 min-1)
15
10
5
0
0
50
100
150
200
250
[3H] Taurine (μM)
III:3
III:4
IV:1
IV:3
B
III:3
IV:3
IV:1
III:4
SLC6A6
TFRC
93
72
31
C
Surface Expression (% III:3, normalized to surface TFRC)
100
50
0
III:3
III:4
IV:1
IV:3
Fibroblasts

Figure 3

A

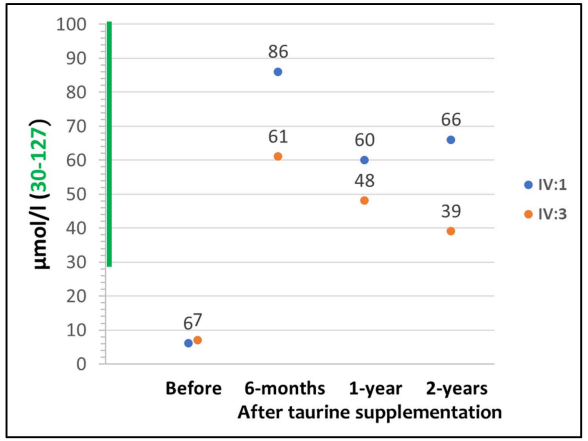

B

	Heart function parameters	Before treatment	1-year of treatment	2-years of treatment
IV:1	LVESD (20-37mm)	38	41	35
	LVEDD (35-56mm)	52	56	52
	EF (55-75%)	48%	50%	55%
	FS (30-40%)	26.8%	27%	32%
IV:3	LVESD (17-25mm)	26	26	25
	LVEDD (29-39mm)	34	36	37
	EF (55-75%)	45%	52%	65%
	FS (30-40%)	23.8%	27.7%	32%

C

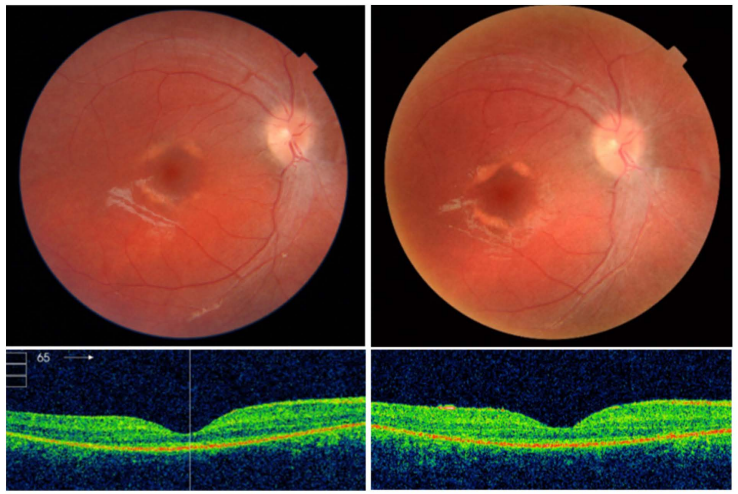

Before treatment 2-years of taurine suppl.

Right eye

D

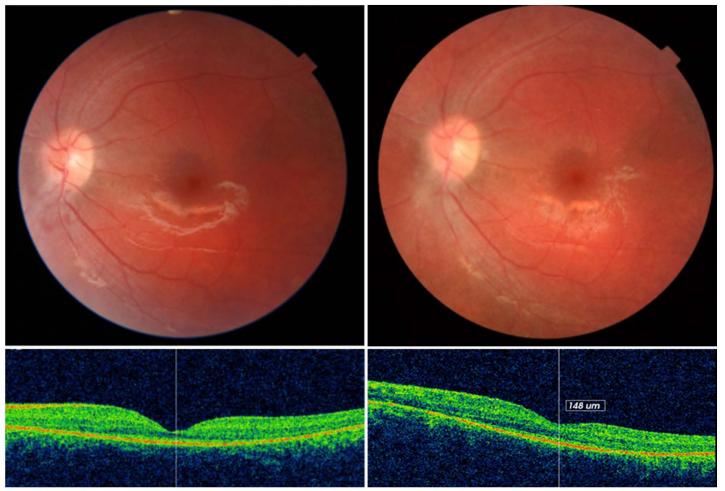

Before treatment 2-years of taurine suppl.

Left eye

Taurine treatment of retinal degeneration and cardiomyopathy in a consanguineous family with SLC6A6 taurine transporter deficiency

Muhammad Ansar[1,2,*,§], Emmanuelle Ranza[1,3,4,*], Madhur Shetty[5], Sohail A. Paracha[6], Maleeha Azam[7], Ilse Kern[8], Justyna Iwaszkiewicz[9], Omer Farooq[10], Constantin J. Pournaras[11], Ariane Malcles[12], Mateusz Kecik[12], Carlo Rivolta[13,14,15], Waqar Muzaffar[16], Aziz Qurban[16], Liaqat Ali[7], Yacine Aggoun[17], Federico A. Santoni[1,18], Periklis Makrythanasis[1,19], Jawad Ahmed[6], Raheel Qamar[7], Muhammad T. Sarwar[6], L. Keith Henry[5], Stylianos E. Antonarakis[1,3,20,§]

[1]Department of Genetic Medicine and Development, University of Geneva, Geneva, Switzerland;

[2]Current address, Clinical Research Center, Institute of Molecular and Clinical Ophthalmology Basel (IOB), Basel, Switzerland;

[3]Service of Genetic Medicine, University Hospitals of Geneva, Geneva, Switzerland;

[4]Current address, Medigenome, Swiss Institute of Genomic Medicine, Geneva, Switzerland;

[5]Dept. of Biomedical Sciences, School of Medicine and Health Sciences, University of North Dakota, Grand Forks, ND, United States;

[6]Institute of Basic Medical Sciences, Khyber Medical University, Peshawar, Pakistan;

[7]Department of Biosciences, Faculty of Science, COMSATS University Islamabad, Pakistan;

[8]Pediatric Nephrology and Metabolism Unit, Pediatric Subspecialties Service, Children's Hospital, Geneva University Hospitals, Geneva, Switzerland;

[9]Swiss Institute of Bioinformatics, Molecular Modeling Group, University of Lausanne, Lausanne, Switzerland;

[10]Bahria University Medical and Dental College, Karachi, Pakistan;

[11]Hirslanden Clinique La Colline, Geneva, Switzerland ;

[12]Department of Ophthalmology, University Hospitals of Geneva, Geneva, Switzerland;

[13]Clinical Research Center, Institute of Molecular and Clinical Ophthalmology Basel (IOB), Basel, Switzerland;

[14]Department of Ophthalmology, University Hospital Basel, Switzerland;

[15]Department of Genetics and Genome Biology, University of Leicester, Leicester, United

[16]Armed Forces Institute of Ophthalmology, Rawalpindi, Pakistan;

[17]Pediatric Cardiology, Geneva University Hospitals, Geneva, Switzerland;

[18]Current address, Department of Endocrinology Diabetes and Metabolism, University Hospital of Lausanne, Lausanne, Switzerland;

[19]Current address, Biomedical Research Foundation of the Academy of Athens, Athens, Greece;

Kingdom;

[20]iGE3 Institute of Genetics and Genomics of Geneva, Geneva, Switzerland;

[*]These authors contributed equally

[§]Corresponding authors;

Muhammad Ansar, muhammad.ansar@unige.ch

Stylianos Antonarakis, stylianos.antonarakis@unige.ch

Supplementary Appendix

Table of Contents

Methods

Genetic analysis

The initial analysis was done by performing the exome sequencing of the proband (IV:3) by using SureSelect Human All Exon v6 reagents (Agilent Technologies, Santa Clara, CA, USA). The sequencing was performed on an Illumina HiSeq4000 platform. A customized pipeline was used to analyze the exome sequencing data, that includes the published algorithms, Burrows-Wheeler aligner tool (BWA)(1), SAMtools(1), PICARD and the Genome Analysis Toolkit (GATK)(2), and the sequenced reads were aligned to the GRCh37/hg19(3) reference human genome. The filtering and interpretation of the filtered variants was performed as described in previous studies(4, 5). All the family members including affecteds (IV:1 and IV:3), unaffected siblings (IV:4 and IV:5) and both parents (III:3 and III:4) were genotyped by using the Illumina 720K SNP array (HumanOmniExpress Bead Chip by Illumina Inc®, San Diego, CA, USA) (Figure 1). PLINK(6) was used to analyze the genotyping data and to calculate the run of homozygosity (ROH). A ROH was defined as the region of 50 consecutive homozygous SNPs, allowing a maximum of one mismatch and bordered by the first heterozygous SNP at the edge.

Molecular modeling of the SLC6A6 missense variant

To predict the potential structural consequences of the SLC6A6 Gly399Val variant, the dopamine transporter structure with bound cocaine molecule (PDB 4xp4) template was used. The UCSF Chimera software(7) was used to model SLC6A6 protein with (Gly399Val) or without (Gly399) variants, and to visualize the resulting protein structures.

Cell and fibroblast Culture

Human embryonic kidney (HEK-293) cell lines were transfected with standard TransIT-LT1 protocol to stably express either wildtype taurine transporter SLC6A6 (formerly called TauT) or a SLC6A6 containing the SNP G399V. Cells and primary fibroblasts were maintained in Dulbecco's Modified Eagle's medium (DMEM), 10% Fetal Bovine Serum (FBS), 1% PSA Antibiotic solution (10,000 units of penicillin, 10,000 µg of streptomycin, and 25 µg of Amphotericin B per mL) at 37˚C and 5% CO2 and were typically used for experiments after reaching 60%-70% confluency.

[^{3}H Taurine] Uptake Assay

HEK-293 cells transiently transfected or stably expressing SLC6A6 or the G399V mutation (100,000 cells/well) or primary fibroblasts (50,000 cells/well) were plated in a 24 well culture plate (culturplate-24, Perkin-Elmer, Inc) and grown for 24 h. Cells were washed twice with 0.5 mL KR buffer (130 mM NaCl, 1.3 mM KCl, 2.2 mM CaCl2, 1.2 mM MgSO4, 1.2 mM KH2PO4, 10 mM HEPES, and 10 mM glucose, pH 7.4.) KR buffer of pH 5.5 was used to perform uptakes as SLC6A6 is more active under acidic conditions. Single point uptake of 30 nM or 5 µM [3H] taurine (Perkin Elmer) with vehicle or indicated concentrations of cold taurine was carried out for 10 minutes at 37˚C. 5 µM was obtained by mixing [3H] taurine with non-labeled taurine. Uptake was terminated with three washes of ice-cold KR buffer of pH 7.4. Radioactivity remaining in cells was measured by liquid scintillation. Non-specific uptake was determined for HEK-293 cells by subtracting radioactivity obtained with parental, non-transfected cells. Non-specific uptake for primary fibroblasts was determined by uptake in the presence of 25 mM non-labeled β-alanine. For

saturation analysis, [^{3}H] taurine was diluted into non-labeled taurine to obtain the necessary concentrations. Uptake was performed for 10 min followed by wash with cold-KR. Non-specific counts were determined as above. Statistical significance was determined using unpaired T-Test and one-way ANOVA (post-Tukey Test) with significance set at $p < 0.05$.

Surface Biotinylation

HEK-293 cells stably expressing SLC6A6 and G399V mutation (100,000 cells/plate) or primary fibroblasts (100,000 cells/plate) were plated in a 100 mM culture plate. At 70% confluency, primary fibroblasts were treated with 50 mM NaCl (final concentration) to enhance SLC6A6 expression. After 12-17 h incubation, all remaining steps were performed on ice to prevent trafficking. Surface SLC6A6 levels were isolated by treatment with 0.5 mg/mL Sulfo-NHS-SS-biotin (ThermoFisher, USA) for 25 minutes upon gentle shaking or rocking. Unreacted biotin was quenched by incubation with 100 mM glycine for 25 minutes with gentle rocking. Cells were solubilized with 500 µL RIPA buffer plus protease inhibitors for 15 minutes on ice. Lysed cells were spun for 20 minutes at 4˚C at 16,000 x g followed by collection of the supernatant. Cells were washed in between biotinylation, quenching and lysing twice with 1X Phosphate-buffered saline with Ca and Mg (PBS/CM) that contained (in mM): 137 mM NaCl, 2.7 mM KCl, 10.1 mM Na2HPO4, 1.8 mM KH2PO4, 0.1 mM CaCl2, 1.0 mM MgCl2, and 10 mM glucose, pH 7.4. 100 µg protein was reacted with 50% slurry neutrAvidin agarose beads (ThermoFisher) and rotated overnight at 4˚C. Beads are then pelleted at 300 x g for 2 minutes and washed with RIPA buffer three times. Beads are incubated with 2X loading dye for 30 minutes at 37˚C, followed by elution of proteins by pelleting the beads at 5,000 x g for 2 minutes. Purified proteins were resolved on

NEXTGEL® 10% acrylamide gels and transferred to 0.45 µM PVDF membranes (Immobilon-P, Millipore). Membranes were blocked for 2 hours at 5% bovine serum albumin (BSA) followed by incubation with SLC6A6 anti-rabbit polyclonal antibody (PA5-37460 Thermo Fisher Scientific) or chicken polyclonal anti-transferrin receptor (TFRC) primary antibody overnight at 4˚C. Membranes were incubated with HRP-conjugated goat anti-rabbit or goat anti-chicken secondary antibody for 1 hour at room temperature. Membranes were imaged on a LiCor C-Digit using WesternSure® PREMIUM Chemiluminescent Substrate (LiCor). SLC6A6 was normalized to TFRC for each membrane sample. Statistical significance was determined using one-way ANOVA (post-Tukey Test) with significance set at $p < 0.05$.

Taurine loading test and supplementation

A taurine loading test was performed in the Pediatrics clinical research unit of the University hospitals of Geneva after approval by the ethics committee. We have administered an oral bolus dose of 100mg/kg of Taurine to the two affected individuals and their heterozygous parents on day 2, this dose was recommended by the literature as non-toxic. Taurine was provided in tablets, commercialized by Burgerstein Pharmaceuticals. Repeated measurements of taurine in blood and urine were subsequently performed. On days 3 and 4, the patients received a 100mg/kg/day, administered in 3 doses (33mg/kg/q8hours).

Results

Genetic analyses reveal a missense variant in the taurine transporter SLC6A6

The genetic analysis was initiated by performing exome sequencing of proband (IV:3) of family F315. More than 95% of the sequenced region was covered at 20x with a total mean coverage of ~100x. An in-house pipeline and prioritization algorithm(4, 5) was used to analyze the high throughput sequencing data. None of the genes known to be implicated in retinal degeneration and all types of visual impairment has yielded any pathogenic variant. Then by combining the exome sequencing data of the proband and genotyping data of all family members, variants present in the regions of homozygosity (ROH) that segregated with the disease phenotype in recessive manner were selected and filtered as described previously(5, 8). By using this approach a homozygous missense variant (NM_003043.5:c.1196G>T:p.(Gly399Val) in *SLC6A6* was identified (Figure 1). The variant SLC6A6:p.(Gly399Val) is not present in gnomAD, Bravo database (https://bravo.sph.umich.edu/freeze5/hg38/) or our local cohort of 300 controls from the same Pakistani ethnicity. As shown in the chromatograms (figure 1B), both the affected individuals (IV:1 and IV:3) are homozygous, both parents (III:3 and III:4) and one unaffected sibling (IV:4) are heterozygous for the variant (Gly399Val) and another unaffected sibling (IV:5) has both normal alleles; confirming the recessive inheritance of the variant. By sharing our findings through GeneMatcher(9), genetic conferences and meetings, we have not found any second case having pathogenic or likely pathogenic variants in the *SLC6A6* gene. However, by publishing this article we hope to identify similar cases.

Clinical evaluation

The two affected individuals and their parents were clinically evaluated at the University Hospital of Geneva. The results of the evaluation are described in the table 1.

Figure S1. Fundus photographs and macular OCT (optical coherence tomography) before taurine supplementation

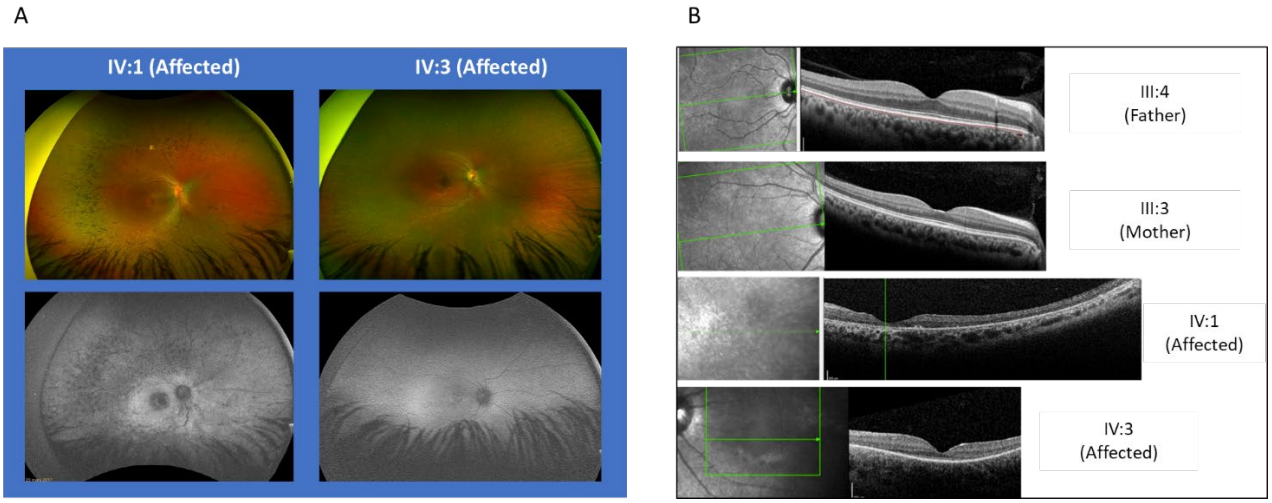

Figure S1. Fundus photographs and macular OCT (optical coherence tomography) before taurine supplementation. (A) Fundus photographs of affected individuals (IV:1 and IV:3) of family F315. (B) OCT is normal in father (III:4) and mother (III:3), uniformly atrophic in affected boy (IV:1) and showing paracentral foveal-spearing photoreceptor atrophy in the affected girl (IV:3).

Plasma and urine amino acids and % kidney tubular reabsorption (tables S2 to S5)

The tables below show the extremely low levels of taurine in the two affecteds (individuals IV:1 and IV:3) and intermediate levels for the carrier parents (individuals III:3 and III:4). A negative value for the renal tubular reabsorption of taurine was observed in the patients, while in the parents these reabsorption values were less than the normal controls.

Table S2. Plasma and urine amino acid levels and % kidney tubular reabsorption in the affected individuals IV:3

Amino acid Affected (IV:3)	Plasma (µmol/l)	Plasma reference values in children (µmol/l)	Urine (mmol/molCreat)	% renal tubular reabsorption
Taurine	5	20 to 90	190	-60
Threonine	72	31 to 30	14	99
Serine	126	25 to 170	106	96
Asparagine	48	-	11	99
Glutamate	24	25 to 250	3	99
Glutamine	607	60 to 470	81	99
Proline	252	50 to 190	368	94
Glycine	226	60 to 310	1182	78
Alanine	228	100 to 310	27	100
Citrulline	17	10 to 30	2	100
Valine	142	60 to 260	5	100
Cystine	28	25 to 65	8	99
Methionine	20	5 to 30	0	100
Isoleucine	45	25 to 95	2	100
Leucine	78	45 to 155	3	100
Tyrosine	45	10 to 120	12	99
Phenylalanine	39	20 to 70	8	99
Ornithine	33	10 to 110	1	100
Lysine	117	45 to 145	11	100
Histidine	66	25 to 110	57	96
Arginine	78	10 to 65	2	100

Table S3. Plasma and urine amino acid levels and % kidney tubular reabsorption in the affected individuals IV:1

Amino acid Affected (IV:1)	Plasma (µmol/l)	Plasma reference values in adults (µmol/l)	Urine (mmol/molCreat)	% renal tubular reabsorption
Taurine	7	40 to 280	213	-110
Threonine	165	100 to 190	14	99

Serine	194	70 to 160	54	98
Asparagine	64		6	99
Glutamate	24	25 to 90	2	99
Glutamine	684	550 to 830	41	100
Proline	507	100 to 380	2	100
Glycine	396	150 to 320	90	98
Alanine	408	240 to 600	19	100
Citrulline	31	20 to 55	1	100
Valine	202	180 to 325	4	100
Cystine	36	40 to 75	7	99
Methionine	31	20 to 45	1	100
Isoleucine	70	50 to 120	1	100
Leucine	115	105 to 215	2	100
Tyrosine	63	40 to 100	9	99
Phenylalanine	58	45 to 80	4	100
Ornithine	41	30 to 100	1	100
Lysine	167	135 to 260	11	100
Histidine	75	65 to 110	46	96
Arginine	109	35 to 140	1	100

Table S4. Plasma and urine amino acid levels and % kidney tubular reabsorption in father (III:4)

Amino acid Father (III:4)	Plasma (µmol/l)	Plasma reference values in adults (µmol/l)	Urine (mmol/molCreat)	% renal tubular reabsorption
Taurine	28	40 to 280	67	79
Threonine	135	100 to 190	9	99
Serine	102	70 to 160	36	97
Asparagine	52		5	99
Glutamate	27	25 to 90	1	100
Glutamine	629	550 to 830	30	100
Proline	389	100 to 380	1	100
Glycine	296	150 to 320	229	93
Alanine	489	240 to 600	22	100
Citrulline	37	20 to 55	1	100
Valine	216	180 to 325	2	100
Cystine	49	40 to 75	7	99
Methionine	28	20 to 45	0	100
Isoleucine	75	50 to 120	1	100
Leucine	127	105 to 215	1	100
Tyrosine	71	40 to 100	7	99
Phenylalanine	66	45 to 80	4	99
Ornithine	58	30 to 100	1	100

Lysine	157	135 to 260	8	100
Histidine	69	65 to 110	30	96
Arginine	85	35 to 140	1	100

Table S5. Plasma and urine amino acid levels and % kidney tubular reabsorption in mother (III:3)

Amino acid Mother (III:3)	Plasma (µmol/l)	Plasma reference values in females (µmol/l)	Urine (mmol/molCreat)	% renal tubular reabsorption
Taurine	31	30 to 55	87	83
Threonine	197	75 to 235	20	99
Serine	152	70 to 185	57	98
Asparagine	62		9	99
Glutamate	25	20 to 70	1	100
Glutamine	607	440 to 810	49	100
Proline	248	70 to 270	1	100
Glycine	358	70 to 530	408	93
Alanine	400	200 to 550	28	100
Citrulline	38	15 to 55	1	100
Valine	188	150 to 270	3	100
Cystine	45	30 to 80	7	99
Methionine	28	20 to 40	0	100
Isoleucine	56	40 to 90	1	100
Leucine	107	75 to 170	2	100
Tyrosine	64	35 to 90	9	99
Phenylalanine	57	40 to 70	7	99
Ornithine	50	20 to 90	1	100
Lysine	192	115 to 250	12	100
Histidine	71	55 to 110	47	96
Arginine	117	25 to 125	1	100

Functional analysis

Functional analysis were performed to observe the effect of the SLC6A6 G399V variant on the taurine uptake and surface expression of the transporter[10].

Figure S2. Taurine uptake in HEK-293 cells expressing the SLC6A6 G399V variant at high and low substrate concentrations

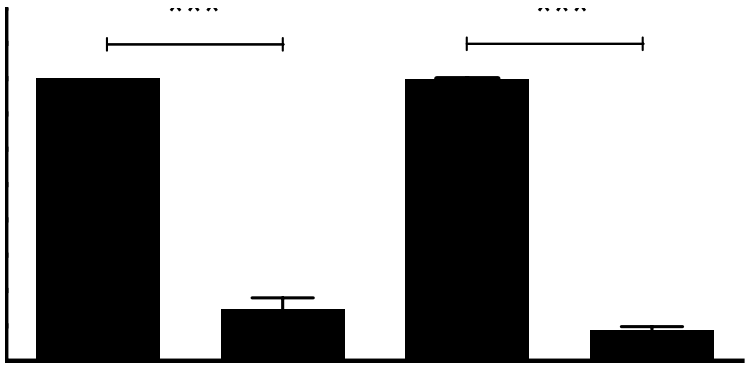

Figure S2. Taurine uptake in HEK-293 cells expressing the SLC6A6 G399V variant at high and low substrate concentrations. HEK-MSR cells were transiently transfected with pcDNA3.1-SLC6A6 or pcDNA3.1- SLC6A6 G399V and analyzed for taurine uptake for 25 min at 37˚C using 30 nM and 5 µM [3H] taurine. Radioactivity incorporated into the cell was determined by scintillation counting and normalized to percent uptake by wild type SLC6A6. Background counts were determined from uptake in a non-transfected cell and were subtracted from test samples. N>3. Significance was determined by unpaired t-test. ***p<0.001.

Figure S3. Taurine Saturation Uptake Analysis of SLC6A6 G399V Mutant in HEK-293 Cells.

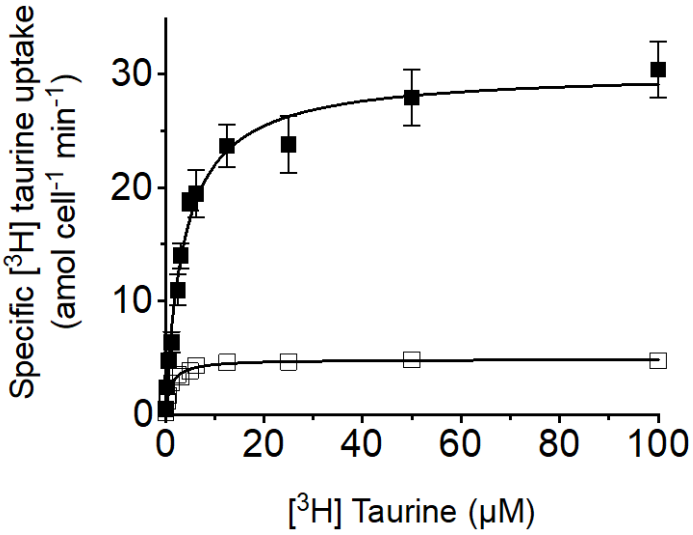

Figure S3. Taurine Saturation Uptake Analysis of SLC6A6 G399V Mutant in HEK-293 Cells. HEK-293 cells were transiently transfected with pcDNA3.1 containing SLC6A6 (filled square) or SLC6A6 G399V (open square) and incubated with [^{3}H]taurine concentrations from 0.05 to 100 μM for 10 min. Endogenous SLC6A6 expression was subtracted using uptake values from non-transfected parental HEK-293 cells.

Table S6. Kinetic Analysis of Taurine uptake by SLC6A6 G399V Mutant

	K_M (μM)	V_{max} (amol/cell/min)
SLC6A6	3.8 ± 0.31	30 ± 1.11
SLC6A6 G399V	1.1 ± 0.05**	4.9 ± 0.24****

Two-tailed unpaired t test, ** P<0.01, **** P<0.0001.

Figure S4. Taurine Uptake in Patient-derived Fibroblasts.

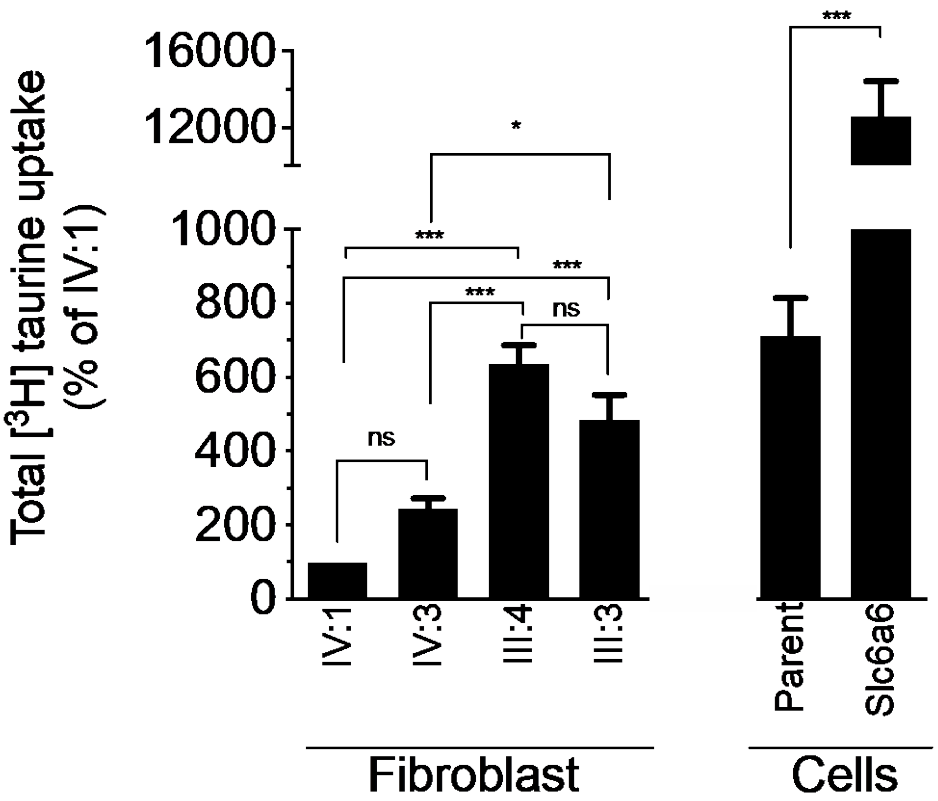

Figure S4. Taurine Uptake in Patient-derived Fibroblasts. Percent uptake is plotted after normalization to IV:1. One-way ANOVA with Tukey's multiple comparison post-hoc. All differences within fibroblast samples were significant at * $p<0.05$, *** $p<0.001$. Nonsignificant differences were indicated by ns. HEK-293 cells were used as a positive control as transfection with SLC6A6 plasmid shows significant ~12-fold increase in taurine transport over the endogenous SLC6A6 transport. 30 nM of [3H] taurine was used for the uptake analysis.

Table S7. Kinetic Analysis of Taurine Uptake by Patient-derived Fibroblasts

	K_M (μM)	V_{max} (amol/cell/min)
IV:1	15.5 ± 2.9	5.33 ± 0.36***
IV:3	15.0 ± 1.7	6.17 ± 0.79***
III:4	11.8 ± 3.5	12.3 ± 1.0###
III:3	24.8 + 5.6	13.37 ± 0.95###

One-way ANOVA with Tukey post hoc test. *** P<0.001 significance from III:4 and III:3. ###P<0.001 significance from IV:1 and IV:3.

Figure S5. SLC6A6 Surface Expression from Transfected Tissue Culture Cells

A **B**

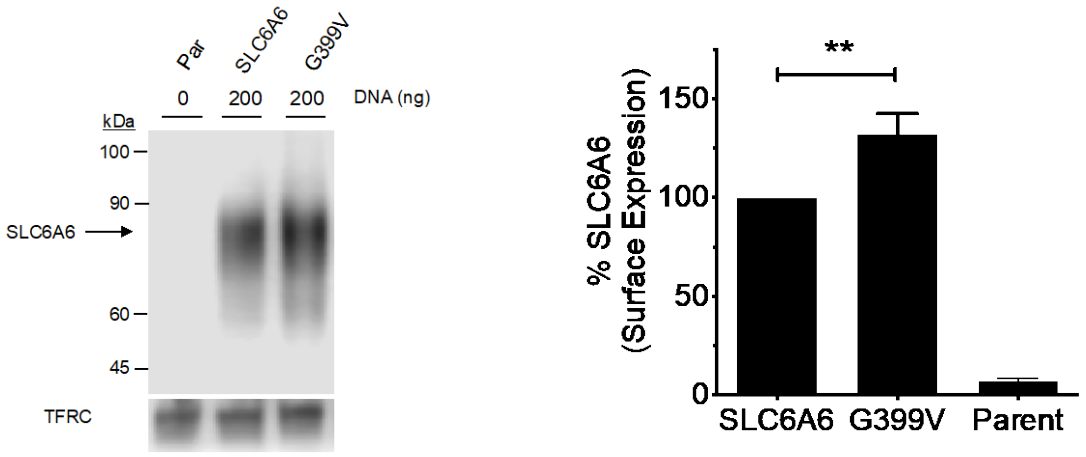

SLC6A6 Surface Expression Analysis in Transiently Transfected HEK-293 Cells. (A) Western blot detection of SLC6A6 from purified plasma membrane biotinylated proteins extracted from parental HEK-293 cells (Par) and cells transiently transfected with 200 ng of plasmid DNA allowing expression of SLC6A6 or SLC6A6 G399V. Blots were striped and probed for the plasma membrane transferrin receptor which was used to normalize SLC6A6 expression. (B) Plot of densitometry values for SLC6A6 normalized to percent of transferrin receptor (TFRC). ** $P<0.01$

Taurine loading test

A baseline profile of taurine levels in blood and urine was first measured in both affected children and their parents; serial measurements without taurine supplementation were obtained during day 1. The results showed extremely low levels of taurine in the two affected individuals (around 5 μmol/l), while their heterozygous parents had intermediate levels. The standard daily diet did not increase the blood taurine levels in the patients or their parents (see Figure S9, day 1).

The results were as follows (figure S9):

- In the two affected children and their parents, blood taurine levels reached a high peak (400-900 μmol/l) after 4 hours; after 8 hours, the levels were still elevated (> 100 μmol/l).
- The kinetics of blood taurine levels were similar between the patients and their parents. Moreover, the time of the peak of blood Taurine levels after the bolus administration was comparable to that of normal volunteers.
- On days 3 and 4, we observed that the taurine supplementation 3 times a day in the affecteds, resulted in a peak of around 250 μmol/l. More importantly, even though the last administration of taurine was at 8pm, the fasting levels in the next morning were between 53 and 78 μmol/l, which correspond to the usual heterozygous levels without supplementation or the low normal range.

Figure S6. Taurine loading test.

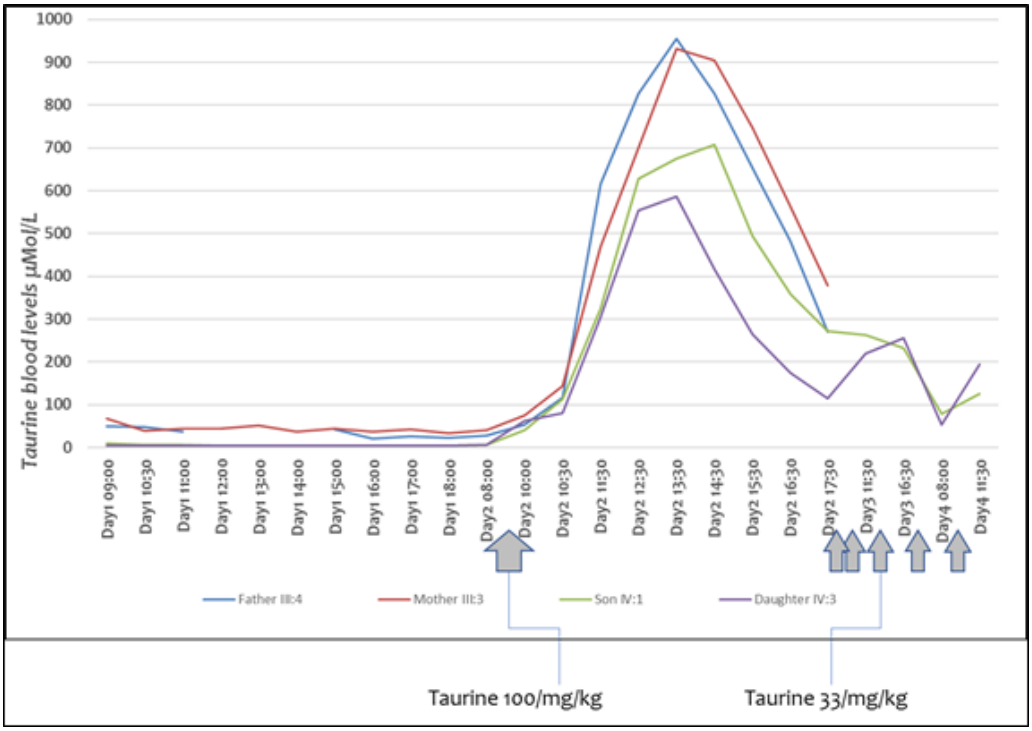

Figure S6. Taurine loading test. Blood Taurine levels in the 4 members of the family, before and after the Taurine loading test, and the Taurine supplementation, performed at the University Hospitals of Geneva. For discussion of the results see text.

Figure S7. Plasma taurine levels in healthy volunteers.

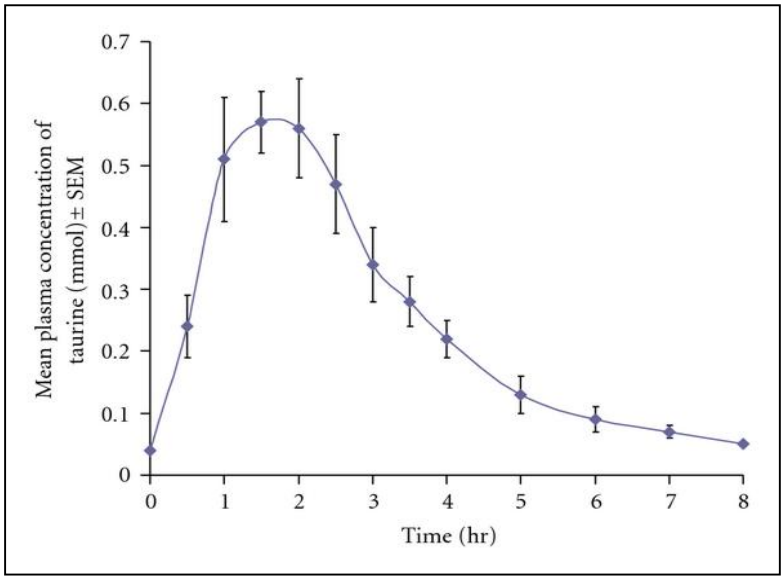

Figure S7. Plasma taurine levels in healthy volunteers. Linear plot of mean plasma taurine levels (mmoL) in eight healthy volunteers following administration of 4 g (32 mmoL) oral taurine (this dose is about half of that used in the members of the F315 family). Data from Ghandforoush-Sattari M et al(11).

These results show that daily supplementation of taurine is sufficient to increase taurine to low normal blood levels: thus, since the mutation in these patients allows a 10-18% intracellular transport of taurine, the increased levels in blood could provide sufficient taurine transport in the retina cells and prevent further destruction of photoreceptors in the affected female. Moreover, this supplementation could avoid progression of the cardiomyopathy in both affected children.

Taurine supplementation and 2 year follow up

Figure S8. Fundus photographs and OCT of boy (IV:1) after two years of taurine supplementation.

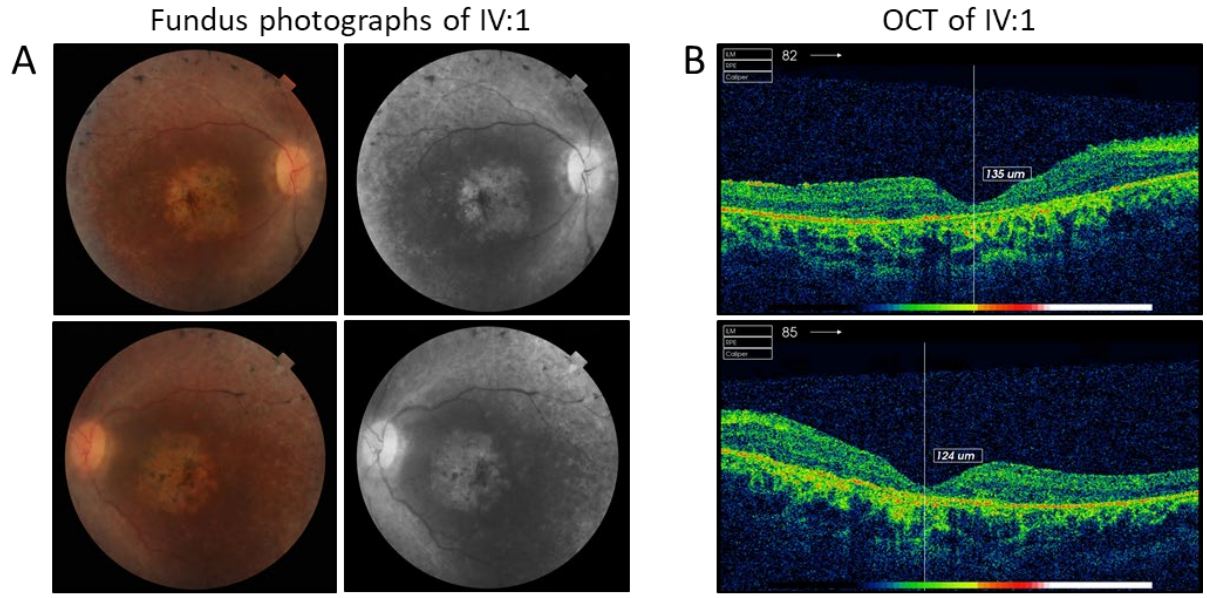

Figure S8. Fundus photographs and OCT of boy (IV:1) after two years of taurine supplementation.

(A) Fundus photographs (A) and OCT (B) of the affected individual (IV:1) of family F315. Results show anatomic stability of the macula; uniformly atrophic in affected boy (IV:1).

Figure S9. Fundus photographs and OCT of the affected girl (IV:3) before the taurine supplementation.

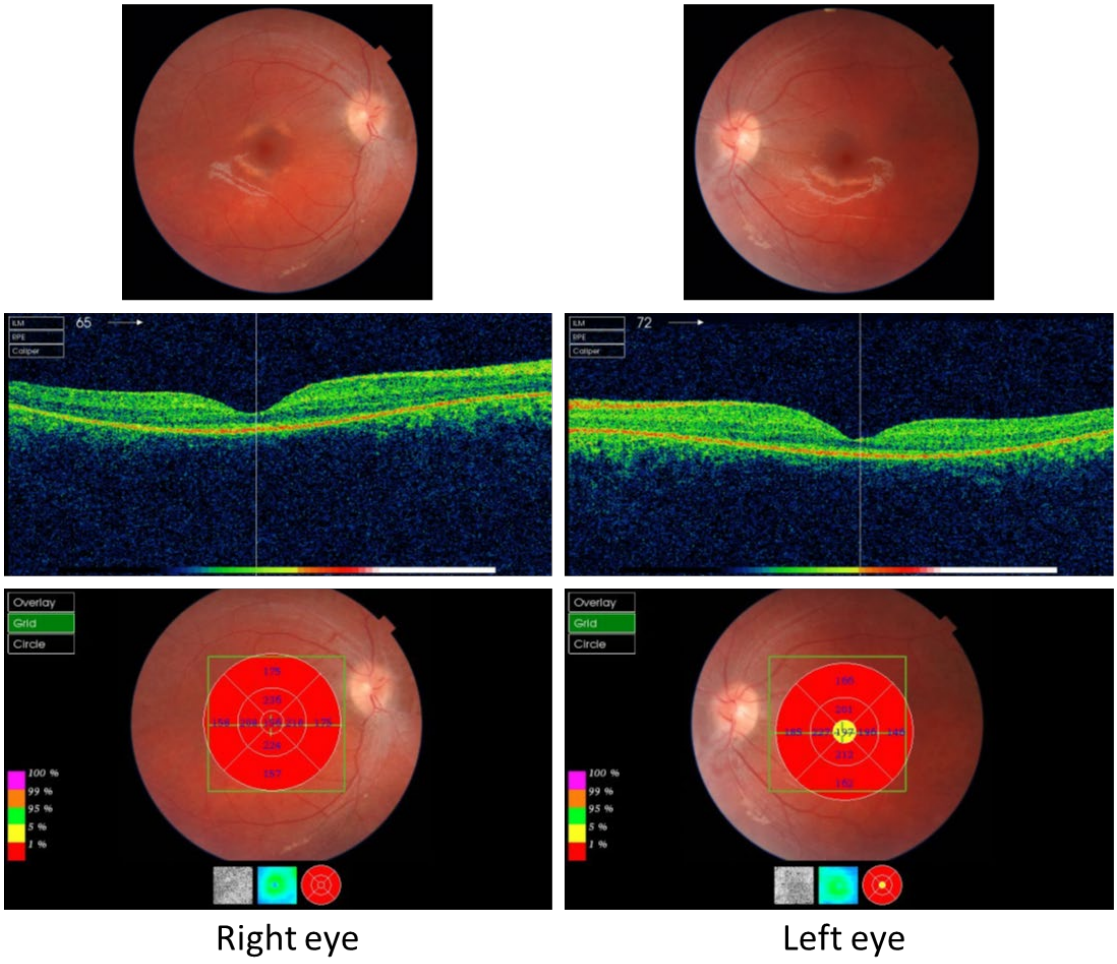

Figure S9. Fundus photographs and OCT of the affected girl (IV:3) before the taurine supplementation. Fundus photographs and OCT of affected girl (IV:3) of family F315 show a paracentral foveal-spearing photoreceptor atrophy in the affected girl (IV:3)

Figure S10. Fundus photographs and OCT of the affected girl (IV:3) 1-year after the taurine supplementation.

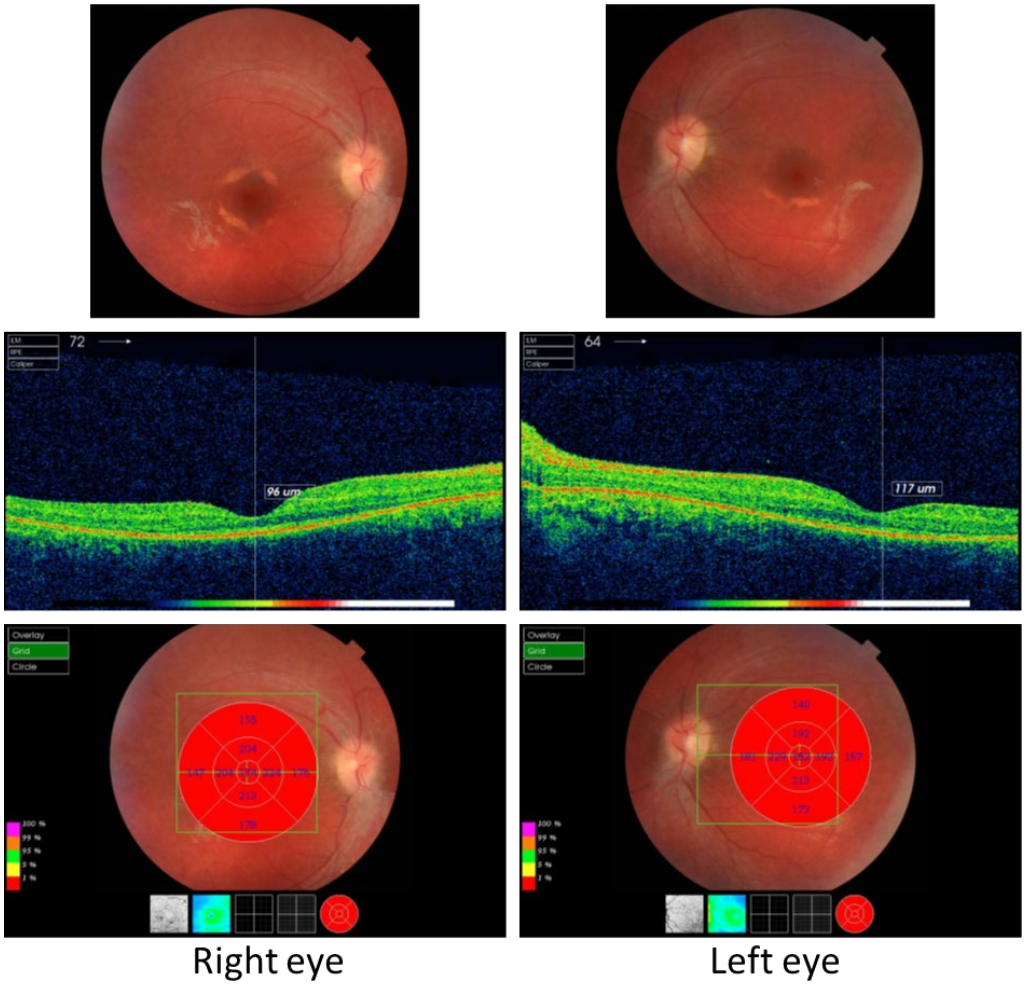

Figure S10. Fundus photographs and OCT of the affected girl (IV:3) 1-year after the taurine supplementation. Fundus photographs and OCT of affected girl (IV:3) show the anatomical stability with preservation of foveal photoreceptors.

Figure S11. Fundus photographs and OCT of the affected girl (IV:3) 2-year after the taurine supplementation.

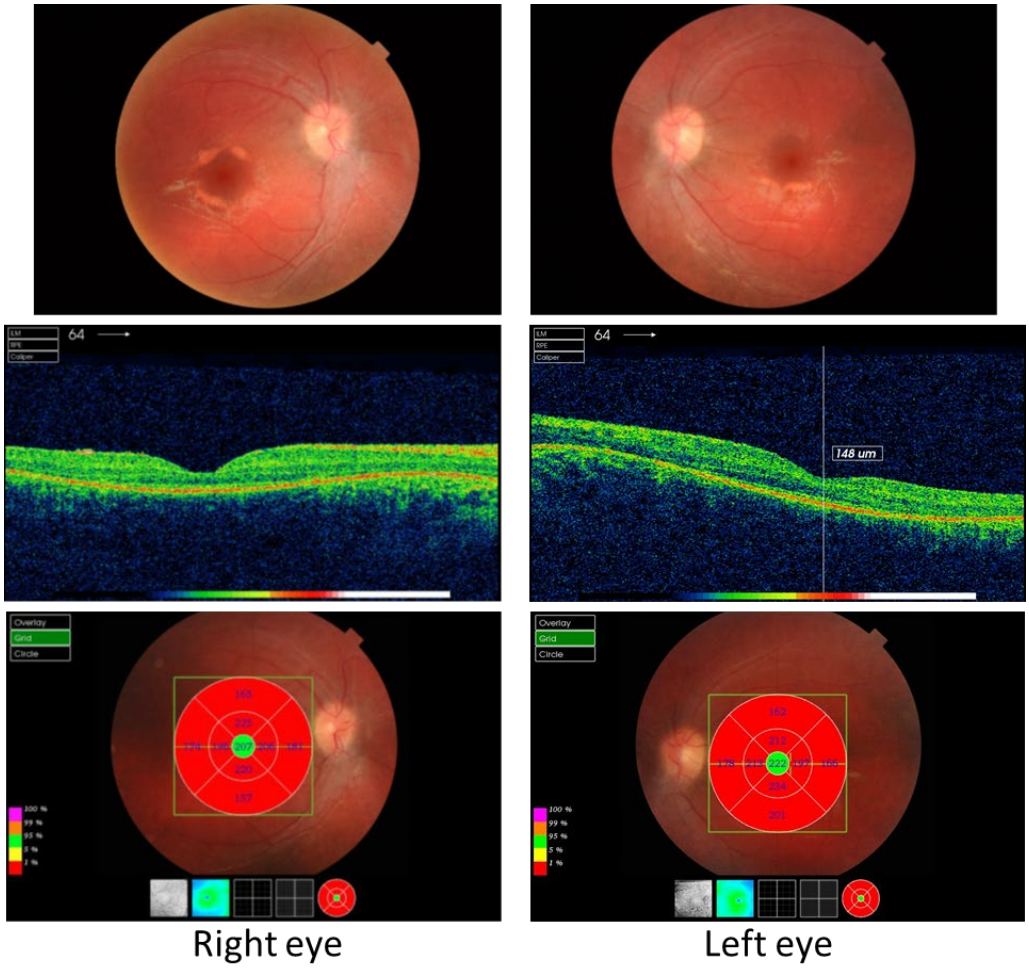

Figure S11. Fundus photographs and OCT of the affected girl (IV:3) 2-year after the taurine supplementation. Fundus photographs and OCT of affected girl (IV:3) show the anatomical stability with preservation of foveal photoreceptors. Her brother (IV:1) had complete visual loss at this age.

Figure S12. Multifocal ERG before and after one and two-years of taurine supplementation.

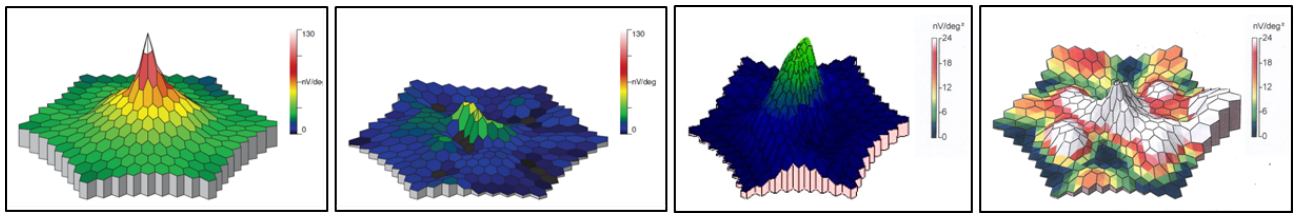

Figure S12. Multifocal ERG before and after one and two-years of taurine supplementation. Multifocal ERG of the patient (IV:3) showing diminished but residual response in the macular region before and after the taurine supplementation.

References

1 Li, H. and Durbin, R. (2009) Fast and accurate short read alignment with Burrows-Wheeler transform. *Bioinformatics*, **25**, 1754-1760.

2 DePristo, M.A., Banks, E., Poplin, R., Garimella, K.V., Maguire, J.R., Hartl, C., Philippakis, A.A., del Angel, G., Rivas, M.A., Hanna, M. *et al.* (2011) A framework for variation discovery and genotyping using next-generation DNA sequencing data. *Nat Genet*, **43**, 491-498.

3 Pruitt, K.D., Tatusova, T. and Maglott, D.R. (2007) NCBI reference sequences (RefSeq): a curated non-redundant sequence database of genomes, transcripts and proteins. *Nucleic acids research*, **35**, D61-65.

4 Makrythanasis, P., Nelis, M., Santoni, F.A., Guipponi, M., Vannier, A., Bena, F., Gimelli, S., Stathaki, E., Temtamy, S., Megarbane, A. *et al.* (2014) Diagnostic exome sequencing to elucidate the genetic basis of likely recessive disorders in consanguineous families. *Hum Mutat*, **35**, 1203-1210.

5 Ansar, M., Chung, H., Waryah, Y.M., Makrythanasis, P., Falconnet, E., Rao, A.R., Guipponi, M., Narsani, A.K., Fingerhut, R., Santoni, F.A. *et al.* (2018) Visual impairment and progressive phthisis bulbi caused by recessive pathogenic variant in MARK3. *Hum Mol Genet*, in press.

6 Purcell, S., Neale, B., Todd-Brown, K., Thomas, L., Ferreira, M.A., Bender, D., Maller, J., Sklar, P., de Bakker, P.I., Daly, M.J. *et al.* (2007) PLINK: a tool set for whole-genome association and population-based linkage analyses. *Am J Hum Genet*, **81**, 559-575.

7 Pettersen, E.F., Goddard, T.D., Huang, C.C., Couch, G.S., Greenblatt, D.M., Meng, E.C. and Ferrin, T.E. (2004) UCSF Chimera--a visualization system for exploratory research and analysis. *J Comput Chem*, **25**, 1605-1612.

8 Ansar, M., Ullah, F., Paracha, S.A., Adams, D.J., Lai, A., Pais, L., Iwaszkiewicz, J., Millan, F., Sarwar, M.T., Agha, Z. *et al.* (2019) Bi-allelic Variants in DYNC1I2 Cause Syndromic Microcephaly with Intellectual Disability, Cerebral Malformations, and Dysmorphic Facial Features. *Am J Hum Genet*, **104**, 1073-1087.

9 Sobreira, N., Schiettecatte, F., Valle, D. and Hamosh, A. (2015) GeneMatcher: a matching tool for connecting investigators with an interest in the same gene. *Hum Mutat*, **36**, 928-930.

10 Tomi, M., Tajima, A., Tachikawa, M. and Hosoya, K. (2008) Function of taurine transporter (Slc6a6/TauT) as a GABA transporting protein and its relevance to GABA transport in rat retinal capillary endothelial cells. *Biochim Biophys Acta*, **1778**, 2138-2142.

11 Ghandforoush-Sattari, M., Mashayekhi, S., Krishna, C.V., Thompson, J.P. and Routledge, P.A. (2010) Pharmacokinetics of oral taurine in healthy volunteers. *J Amino Acids*, **2010**, 346237.

Table S1: Clinical features of affected individuals with recessive *SLC6A6* variants.

	15 y.o individual IV:1 of fig 1	**6 y.o. individual IV:3 of fig 1**
General	Height 169cm (+0.5 SD) Weight 48.5kg (-1 SD) HC 51.5cm (-3 SD) Pectus carinatum No dysmorphic features	Height 107cm (-1.5 SD) Weight (-2 SD) HC 46.5cm (-3.5 SD) No dysmorphic features
Neurology	Cranial nerves: normal Muscle tone and strength: normal Reflexes: normal Cerebellar exam: normal *Brain MRI*: normal	Cranial nerves: normal Muscle tone and strength: normal Reflexes: normal Cerebellar exam: normal *Brain MRI*: normal
ENT	Bilateral scars on tympanic membranes *Audiometry*: normal	Bilateral seromucous otitis *Audiometry*: slight decrease (10-20 dB) in low frequencies, of conductive origin

Cardiology	BP: 127/70 mmHg Heart rate: 102/min Saturation: 100% AA No heart murmurs *Echocardiography*: mild hypokinetic cardiomyopathy with systolic dysfunction (shortening fraction 26-27 %) and slight systolic dilatation of left ventricle (Z score +3.2). *Effort test*: normal	BP: 103/73 mmHg Heart rate: 135/min Saturation: 100% AA No heart murmurs *Echocardiography*: mild hypokinetic cardiomyopathy with systolic dysfunction (shortening fraction 24 %) and slight systolic dilatation of left ventricle (Z score +2.5). *Effort test*: normal
Ophthalmology	Visual acuity: Light perception ODS *Fundus*: advanced cone-rod dystrophy, severe peripheral alterations and central atrophy *Autofluorescence*: severe peripheral and central hypoautofluorescence with a preserved paracentral ring of isoautofluorescence *Global electroretinogram (ERG)*: extinguished *Multifocal ERG*: not possible to perform due to complete visual loss *Visual field*: not possible to perform	Visual acuity: Counting fingers ODS *Fundus*: cone-rod dystrophy, salt-and-peper peripheral alterations and paracentral macular atrophy *Autofluorescence*: central area of isoautofluorescence with a ring of hypoautofluorescence and outer ring of hyperautofluorescence; normal autofluorescence in retinal periphery *Global electroretinogramm (ERG)*: extinguished *Multifocal ERG*: minimal foveal macular response *Visual field*: abnormal, paracentral scotoma with a relatively preserved peripheral visual field

	Optic coherence tomography (OCT): extended atrophy of the retina predominantly in the outer layers	*Optic coherence tomography (OCT)*: parafoveal outer retinal and photoreceptor atrophy; preservation of foveal photoreceptors
Hepatic	Transaminases, γGT, bilirubin, PA, albumin and coagulation studies: normal *Abdominal ultrasound with ARFI*: normal; no evidence of hepatic fibrosis	Transaminases, γGT, bilirubin, PA, albumin and coagulation studies: normal *Abdominal ultrasound with ARFI*: normal; no evidence of hepatic fibrosis
Biochemical testing	Very low levels of blood taurine Markedly increase of urinary taurine levels	Very low levels of blood taurine Markedly increase of urinary taurine levels